Visegrád/Hungary, June/July 1999, *Lecture Notes in Computer Science* 1613,
A. Kuba, M. Šámal, and A. Todd-Pokropek (Eds.), Springer-Verlag 1999, 252-265

Approximating Thin-Plate Splines for Elastic Registration: Integration of Landmark Errors and Orientation Attributes

Karl Rohr, Mike Fornefett, and H. Siegfried Stiehl

Universität Hamburg, Fachbereich Informatik, Arbeitsbereich Kognitive Systeme
Vogt-Kölln-Str. 30, D-22527 Hamburg, Germany
rohr@informatik.uni-hamburg.de

Abstract. We introduce an approach to elastic registration of tomographic images based on thin-plate splines. Central to this scheme is a well-defined minimizing functional for which the solution can be stated analytically. In this work, we consider the integration of anisotropic landmark errors as well as additional attributes at landmarks. As attributes we use orientations at landmarks and we incorporate the corresponding constraints through scalar products. With our approximation scheme it is thus possible to integrate statistical as well as geometric information as additional knowledge in elastic image registration. On the basis of synthetic as well as real tomographic images we show that this additional knowledge can significantly improve the registration result. In particular, we demonstrate that our scheme incorporating orientation attributes can preserve the shape of rigid structures (such as bone) embedded in an otherwise elastic material. This is achieved without selecting further landmarks and without a full segmentation of the rigid structures.

1 Introduction

Image registration based on point landmarks plays a major role in, e.g., neurosurgery planning and intraoperative navigation. While rigid and affine schemes can only describe global geometric differences between images, elastic schemes can additionally cope with local differences. Reasons for local geometric differences are different anatomy (or pathology), scanner- or patient-induced distortions, as well as intraoperative deformations due to surgical interventions.

The most widely applied method for point-based elastic image registration is based on thin-plate splines. This approach has been introduced into medical image analysis by Bookstein [2]. Evans et al. [9] applied this scheme to 3D medical images. Thin-plate splines have a physical motivation, are mathematically well-founded, and are moreover computationally efficient. Alternative splines based on the Navier equation, which have been named elastic body splines, have recently been introduced by Davis et al. [7]. Extensions of point-based elastic schemes which allow to include additional attributes at landmarks have been proposed by Bookstein and Green [5] and Mardia and Little [11]. The combination of thin-plate splines with mutual information as similarity measure for the

purpose of refining initially coarsely specified landmarks has been proposed by Meyer et al. [16].

In all of these approaches from above the interpolation case has been treated. This means that corresponding landmarks are forced to match exactly and thus it is (implicitly) assumed that the landmark positions are known exactly. This assumption, however, is unrealistic since landmark extraction is always prone to error. Approximation schemes, on the other hand, allow to incorporate landmark errors. The error information is used to control the influence of the landmarks on the registration result, which is important in clinical applications. Also, the resulting computational scheme is more robust in comparison to an interpolation approach. However, it seems that approximation schemes have so far not been a focus of research (but see Bookstein [3], Rohr et al. [17], and Christensen et al. [6] for exceptions). A more detailed discussion of these schemes is given in Section 2 below.

This contribution is concerned with an approximation scheme for point-based elastic image registration using thin-plate splines. Central to this scheme is a well-defined minimizing functional for which the solution can be stated analytically. Therefore, we yield an efficient computational scheme for determining the transformation between two images. In earlier work, we have introduced an approach that allows to incorporate isotropic as well as anisotropic landmark errors and we have proposed a scheme for estimating landmark localization uncertainties directly from the image data (Rohr et al. [17]–[19]). In this contribution, we suggest a generalization of our work which allows to integrate additional attributes at point landmarks. By this, additional knowledge is used to further improve the registration result without the necessity of specifying additional landmarks. In our case, we consider orientation attributes at corresponding points. Generally, these attributes characterize the local orientation of the contours at the landmarks. In previous work on the incorporation of additional attributes, Bookstein and Green [5] have represented orientations by additional points close to the landmarks, thus they used a finite difference scheme. Mardia and Little [11] have proposed a scheme based on the method of kriging where exact orientations are incorporated. Their scheme requires the orientation vectors to be unit vectors. This imposes constraints which may not be desired. The approach we propose also includes exact orientations, however, in comparison to [11] the orientation vectors need not to be normalized to unit vectors. This is achieved by representing the constraints due to the orientations through scalar products. Additionally, we treat the interpolation as well as the approximation case. In particular, we propose a combined scheme that integrates isotropic as well as anisotropic errors together with orientation attributes. Also, we extend the domain of application of our scheme to the important case of preserving rigid structures (such as bone) embedded in an otherwise elastic material. It seems that this application has so far not gained much attention in previous work on point-based registration using attributes (but see Mardia and Little [11]). In comparison to other schemes such as Little et al. [14] a full segmentation of the rigid structures is not necessary for our approach.

The remainder of this contribution is organized as follows. In the next section, we discuss in more detail related work on approximation schemes for point-based nonrigid image registration. Then, we describe our approach based on thin-plate splines which integrates anisotropic landmark errors and orientation attributes. The applicability of the approach is demonstrated for synthetic data as well as real tomographic images of the human brain.

2 Related Work

In this section, we discuss approximation schemes for point-based nonrigid image registration. For other approaches to medical image registration we refer to a recent review by Maintz and Viergever [15].

In [3], Bookstein proposed an approach to relaxing the original interpolating thin-plate spline approach [2] by straightforward combination of different energy terms, where one term represents the bending energy of interpolating thin-plate splines and the other the distance of the landmark configurations (note, that in total four different energy terms have been proposed which may be combined). The basis of the approach is a linear regression model and the technique is referred to as 'curve décolletage' (Leamer [13]). With this approach it is possible to incorporate isotropic and anisotropic errors. However, since the approach has not been related to a minimizing functional w.r.t. the searched transformation it is generally not clear whether all solutions in the whole function space are obtained. The approach has been described for 2D datasets and experimental results have been reported for 2D synthetic data. The landmarks as well as the corresponding errors have been specified manually.

In [17], we have introduced approximating thin-plate splines for elastic image registration. Our approach is based on the mathematical work of Duchon [8] and Wahba [21] which is a different mathematical framework in comparison to that in Bookstein [3]. The basis is a minimizing functional w.r.t. the searched transformation. The solution in the whole function space can be shown to be unique and can be stated analytically. While in [17] we have treated the case of isotropic errors, in [18],[19] we have recently incorporated anisotropic errors for the landmarks in both of the images to be registered. Also, we have proposed to estimate the landmark localization uncertainties directly from the image data utilizing the Cramér-Rao bound (see [19]). The approach has been applied to 2D as well as 3D tomographic images of the human brain and the landmarks have been localized semi-automatically using differential operators.

Recently, Christensen et al. [6] introduced a hierarchical approach to image registration combining a landmark-based scheme with an intensity-based approach using a fluid model. The landmark scheme is based on the linear elasticity operator, thus the resulting splines are different from thin-plate splines. Another difference to our approach is that the nonaffine part of the transformation is separated from the affine part in their functional. The approach has been applied to the registration of 3D cryosection data of a macaque monkey brain as well to MR images of the human brain. Isotropic landmark errors have been

included in one of the two images to be registered. Since no further details have been given on how the errors have been determined, it seems that equal isotropic errors have been used in their application.

As already mentioned above, Bookstein and Green [5] as well as Mardia and Little [11] introduced nonrigid registration schemes incorporating orientation attributes. These schemes are based on a finite difference scheme and the method of kriging, resp. In both of these works the interpolation case has been treated only, although a generalization to approximation is principally possible.

3 Thin-Plate Splines with Landmark Errors and Additional Attributes

We now describe our approach to elastic image registration based on thin-plate splines. This approach incorporates landmark errors as well as orientation attributes at landmarks. While the landmark errors represent statistical information about the uncertainty of landmark localization, the orientation attributes represent geometric information about the contours at the landmarks. Below, we first briefly review our scheme incorporating anisotropic landmark errors and then describe an extension for incorporating orientation attributes.

3.1 Anisotropic Landmark Errors

We denote the sets of landmarks in two images by $\mathbf{p}_i$ and $\mathbf{q}_i$, $i = 1 \ldots n$, and the transformation that maps two images by $\mathbf{u}$ with components $u_k, k = 1 \ldots d$, where d is the image dimension. The bending energy of thin-plate splines can be written as a function of the order m of derivatives in the functional as well as the image dimension d as

$$J_m^d(\mathbf{u}) = \sum_{k=1}^{d} J_m^d(u_k), \tag{1}$$

where

$$J_m^d(u_k) = \sum_{\alpha_1+\ldots+\alpha_d=m} \frac{m!}{\alpha_1! \cdots \alpha_d!} \int_{\mathbb{R}^d} \left(\frac{\partial^m u_k}{\partial x_1^{\alpha_1} \cdots \partial x_d^{\alpha_d}} \right)^2 d\mathbf{x} \tag{2}$$

according to Duchon [8], Wahba [21]. Under the necessary and sufficient condition of $2m - d > 0$ the functional is bounded.

Anisotropic landmark errors are represented by covariance matrices $\boldsymbol{\Sigma}_i$. In this case the minimizing functional reads as

$$J_\lambda(\mathbf{u}) = \frac{1}{n} \sum_{i=1}^{n} (\mathbf{q}_i - \mathbf{u}(\mathbf{p}_i))^T \boldsymbol{\Sigma}_i^{-1} (\mathbf{q}_i - \mathbf{u}(\mathbf{p}_i)) + \lambda J_m^d(\mathbf{u}) \tag{3}$$

and consists of two terms (see Rohr et al. [18],[19]). The first term measures the distance between the two landmark sets weighted by the covariance matrices

$\boldsymbol{\Sigma}_i$. The second term represents the smoothness of the transformation, and the parameter λ weights the two terms. Special cases of this approximation scheme are interpolating thin-plate splines and optimal affine transformations. The approach is applicable to arbitrary image dimensions d, e.g., 2D and 3D images. For the functional in (3) there exists a unique analytic solution, which can be stated as

$$u_k(\mathbf{x}) = \sum_{\nu=1}^{M} a_{k,\nu}\phi_\nu(\mathbf{x}) + \sum_{i=1}^{n} w_{k,i}U(\mathbf{x},\mathbf{p}_i), \qquad k = 1,...,d, \tag{4}$$

with monomials ϕ up to order $m-1$ and suitable radial basis functions U (see Wahba [21],[22], Wang [23]). The coefficients $\mathbf{a} = (\mathbf{a}_1^T,...,\mathbf{a}_M^T)^T$, $\mathbf{a}_i^T = (a_{1,i},...,a_{d,i})$, and $\mathbf{w} = (\mathbf{w}_1^T,...,\mathbf{w}_n^T)^T$, $\mathbf{w}_i^T = (w_{1,i},...,w_{d,i})$ of the transformation $\mathbf{u}$ can efficiently be computed through the following system of linear equations:

$$\begin{aligned}(\mathbf{K} + n\lambda\mathbf{W}^{-1})\mathbf{w} + \mathbf{P}\mathbf{a} &= \mathbf{v} \\ \mathbf{P}^T\mathbf{w} &= \mathbf{0},\end{aligned} \tag{5}$$

where $\mathbf{W}$ represents the landmark errors by $\mathbf{W}^{-1} = \mathrm{diag}\{\boldsymbol{\Sigma}_1,\ldots,\boldsymbol{\Sigma}_n\}$ and is a block-diagonal matrix. The other matrices in (5) are given by $\mathbf{K} = (K_{ij}\mathbf{I}_d)$, where $K_{ij} = U(\mathbf{p}_i,\mathbf{p}_j)$ and $\mathbf{I}_d$ is the $d \times d$ unity matrix, and $\mathbf{P} = (P_{ij}\mathbf{I}_d)$, where $P_{ij} = \phi_j(\mathbf{p}_i)$. The vector $\mathbf{v}$ can be written as $\mathbf{v} = (\mathbf{v}_1^T,...,\mathbf{v}_n^T)^T$, $\mathbf{v}_i^T = (q_{i,1},...,q_{i,d})$.

Note, that our approximation scheme using covariance matrices is also a generalization of the work in Bookstein [4], where the interpolation case is solved while the landmarks are allowed to slip along straight lines within a 2D image. Actually, this is a special case of our approximation scheme since for straight lines the variance in one direction is zero whereas in the perpendicular direction it is infinite.

3.2 Landmark Errors and Orientation Attributes

The approach described above can further be generalized for inclusion of additional attributes at landmarks. In our case, we incorporate orientation attributes. These attributes characterize the local orientation of the contours at the landmarks and represent additional knowledge for elastic image registration.

At corresponding landmarks we assume to have orientations which we want to match (note, that these landmarks are generally a subset of the overall landmarks). We denote those landmarks in the first and second image by $\mathbf{p}_{\theta_i}$ and $\mathbf{q}_{\theta_i}$ and the corresponding orientations by $\mathbf{d}_i$ and $\mathbf{e}_i$, resp. To define a matching criterion between the orientations, we need the transformed vector of $\mathbf{d}_i$. This vector can be stated as $(\mathbf{d}_i^T\nabla)\mathbf{u}(\mathbf{p}_{\theta_i})$. Now we require that this transformed vector is perpendicular to $\mathbf{e}_{i,k}^{\perp}$, which are the k-th orthogonal vectors to the orientation vector $\mathbf{e}_i$ in the second image. In this case, the scalar product between the vectors is zero, otherwise it is different from zero. Choosing vectors from the orthogonal space has the advantage that the corresponding scalar product

is zero independently of the length of the vectors. This is an advantage over the approach in Mardia and Little [11] (see also Mardia et al. [12]), where the orientation vectors are required to be unit vectors and where the interpolation case has been treated only. In our work, we both treat the interpolation as well as the approximation case. Note, however, that the property of length independence only holds in the case of interpolation, but not for approximation. In general we have $d-1$ perpendicular orientations $\mathbf{e}_{i,k}^{\perp}$ which constrain the orientation of the transformed orientation vector of the first image to lie on a line. If the number of perpendicular orientations is smaller, i.e., the number of constraints is lower, then the orientation of the transformed orientation vector is not constrained w.r.t. a line, but w.r.t. a plane, for example (see also Fornefett et al. [10]).

Having defined the matching criterion between orientations we can now state the generalized minimizing functional using $\boldsymbol{\epsilon}_i = \mathbf{q}_i - \mathbf{u}(\mathbf{p}_i)$ as

$$J_\lambda(\mathbf{u}) = \frac{1}{n}\sum_{i=1}^{n} \boldsymbol{\epsilon}_i^T \boldsymbol{\Sigma}_i^{-1} \boldsymbol{\epsilon}_i + \frac{1}{n_2'}\sum_{i=1}^{n_\theta}\sum_{k=1}^{d-1} \left((\mathbf{d}_i^T\nabla)\mathbf{u}^T(\mathbf{p}_{\theta i})\mathbf{e}_{i,k}^{\perp}\right)^2 + \lambda J_m^d(\mathbf{u}), \quad (6)$$

where $n_2' = n_2/c$, $c > 0$, and $n_2 = n_\theta(d-1)$. In comparison to the functional (3) from above we have an additional term that incorporates the orientation constraints. n_θ is the total number of orientations in each of the images. The parameter c weights the orientation term w.r.t. the term representing the landmark errors and also determines (besides λ) whether we interpolate or approximate the orientations. Note, that we can incorporate an arbitrary number of orientations at each landmark. As described above, the orientation constraints are incorporated by scalar products between the transformed orientations of the first image and orientations perpendicular to the orientations in the second image. The solution to the functional in (6) can be stated as

$$\begin{aligned}\mathbf{u}(\mathbf{x}) = &\sum_{\nu=1}^{M}\sum_{k=1}^{d} a_{k,\nu}\phi_\nu(\mathbf{x})\boldsymbol{\varepsilon}_k + \sum_{i=1}^{n}\sum_{k=1}^{d} w_{1,k,i}U(\mathbf{x},\mathbf{p}_i)\boldsymbol{\varepsilon}_k \\ &- \sum_{i=1}^{n_\theta}\sum_{k=1}^{d-1} w_{2,k,i}(\mathbf{d}_i^T\nabla)U(\mathbf{x},\mathbf{p}_{\theta i})\mathbf{e}_{i,k}^{\perp}, \end{aligned} \quad (7)$$

with monomials ϕ up to order $m-1$ and radial basis functions U as above. $\boldsymbol{\varepsilon}_k$, $k = 1 \ldots d$, are the canonical basis vectors of the $\mathbb{R}^d$. The solution is analogous to (4) from above, but additionally we have a term that represents the orientation constraints. Note, that in order to obtain bounded functionals the used function space has to be constrained. Choosing $m = 2$ for the order of derivatives of the smoothness term, then for both cases of 2D and 3D images ($d = 2, 3$) incorporating orientations, we have the basis function $U(\mathbf{x}) = |\mathbf{x}|^3$. The parameter vectors $\mathbf{a} = (\mathbf{a}_1^T, ..., \mathbf{a}_M^T)^T$, $\mathbf{a}_i^T = (a_{1,i}, ..., a_{d,i})$, and $\mathbf{w} = (\mathbf{w}_{1,1}^T, ..., \mathbf{w}_{1,n}^T, \mathbf{w}_{2,1}^T, ..., \mathbf{w}_{2,n_\theta}^T)^T$, $\mathbf{w}_{1,i}^T = (w_{1,1,i}, ..., w_{1,d,i})$, $\mathbf{w}_{2,i}^T = (w_{2,1,i}, ..., w_{2,d-1,i})$ of the transformation $\mathbf{u}$ can be computed by solving the linear system of equations

$$\begin{aligned}\mathbf{K}\mathbf{w} + \mathbf{P}\mathbf{a} &= \mathbf{v} \\ \mathbf{P}^T\mathbf{w} &= \mathbf{0},\end{aligned} \quad (8)$$

with

$$\mathbf{K} = \begin{pmatrix} \mathbf{K}_1 + n\lambda\mathbf{W}^{-1} & \mathbf{K}_2 \\ \mathbf{K}_3 & \mathbf{K}_4 + n_2'\lambda\mathbf{I}_{n_2} \end{pmatrix} \qquad \text{and} \qquad \mathbf{P} = \begin{pmatrix} \mathbf{P}_1 \\ \mathbf{P}_2 \end{pmatrix}, \tag{9}$$

where $\mathbf{W}^{-1} = \text{diag}\{\boldsymbol{\Sigma}_1, \ldots, \boldsymbol{\Sigma}_n\}$ as in (5) and $\mathbf{I}_{n_2}$ is the $n_2 \times n_2$ unity matrix with $n_2 = n_\theta(d-1)$. The other matrices in (9) are given by $\mathbf{K}_1 = (K_{1,ij}\mathbf{I}_d)$, where $K_{1,ij} = U(\mathbf{p}_i, \mathbf{p}_j)$ and $\mathbf{I}_d$ is the $d \times d$ unity matrix; $\mathbf{K}_2 = (K_{2,ij}\mathbf{F}_j)$, where $K_{2,ij} = -(\mathbf{d}_j^T\nabla)U(\mathbf{p}_i, \mathbf{p}_{\theta_j})$, $F_{j,kl} = \boldsymbol{\varepsilon}_k^T\mathbf{e}_{j,l}^{\perp}$, and $\mathbf{F}_j$ are $d \times (d-1)$ matrices; $\mathbf{K}_3 = \mathbf{K}_2^T$; $\mathbf{K}_4 = (K_{4,ij}\mathbf{E}_{ij})$, where $K_{4,ij} = -(\mathbf{d}_j^T\nabla)(\mathbf{d}_i^T\nabla)U(\mathbf{p}_{\theta_i}, \mathbf{p}_{\theta_j})$, $E_{ij,kl} = (\mathbf{e}_{i,k}^{\perp})^T\mathbf{e}_{j,l}^{\perp}$, and $\mathbf{E}_{ij}$ are $(d-1) \times (d-1)$ matrices; $\mathbf{P}_1 = (P_{1,ij}\mathbf{I}_d)$, where $P_{1,ij} = \phi_j(\mathbf{p}_i)$, and $\mathbf{P}_2 = (P_{2,ij}\mathbf{F}_i^T)$, where $P_{2,ij} = (\mathbf{d}_i^T\nabla)\phi_j(\mathbf{p}_{\theta_i})$. $\mathbf{K}$ and $\mathbf{P}$ are of dimension $n' \times n'$ and $n' \times dM$, resp., with $n' = nd + n_\theta(d-1)$. The vector $\mathbf{v}$ is given by $\mathbf{v} = (\mathbf{v}_1^T, ..., \mathbf{v}_n^T, 0, ..., 0)^T$, $\mathbf{v}_i^T = (q_{i,1}, ..., q_{i,d})$, with n_2 zeros at the end.

4 Experimental Results

We demonstrate the applicability of our approach using synthetic data as well as real tomographic images of the human brain. In the first two experiments we have incorporated either anisotropic landmark errors only or orientation attributes only. For the last two experiments we have integrated both landmark errors (isotropic as well as anisotropic errors) and orientation attributes.

In the first example, we register the 2D MR brain images of different patients displayed in Fig. 1. We have used normal landmarks and quasi-landmarks. The quasi-landmarks have no unique position in comparison to normal landmarks, e.g., arbitrary edge points. The incorporation of quasi-landmarks is important since normal point landmarks are hard to define at the outer parts of the human head. For all landmarks the covariance matrices have been estimated directly from the image data by utilizing the Cramér-Rao bound

$$\boldsymbol{\Sigma}_g = \frac{\sigma_n^2}{m}\mathbf{C}_g^{-1}, \tag{10}$$

where σ_n^2 denotes the variance of additive white Gaussian image noise, m the number of voxels in a local 3D window, and $\mathbf{C}_g = \overline{\nabla g\,(\nabla g)^T}$ is the averaged dyadic product of the image gradient (Rohr [19], van Trees [20]). Note, that the Gaussian noise model is an approximation and that we assume that the dependence of the noise on the signal can be neglected (but see Abbey et al. [1]). In Fig. 1 the landmark localization uncertainties are represented by error ellipses (note, that the ellipses have been enlarged by a factor of 7 for visualization purposes). It can clearly be seen that for the normal landmarks the localization uncertainty is small in all directions, while for the quasi-landmarks (landmarks Nr. 9-12) the localization uncertainty is large along the edge but small perpendicular to it. Fig. 2 on the left shows the registration result when using only the normal landmarks for elastic image registration (landmarks Nr. 1-6 and 8). Here, we have applied our approximating thin-plate spline approach while incorporating isotropic errors and setting $m = d = 2$ in (3). We have transformed

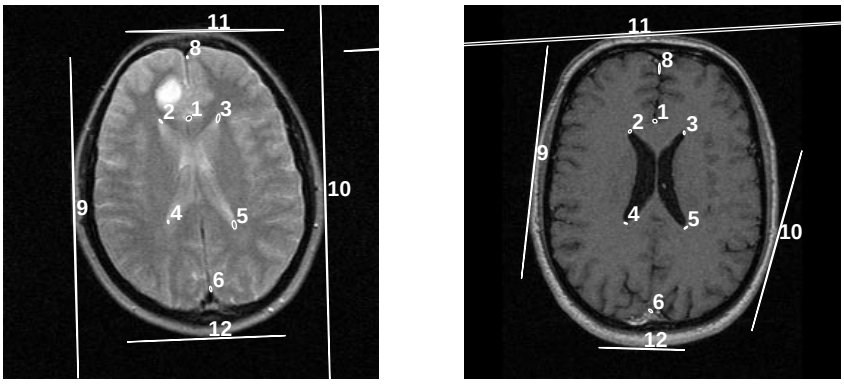

Fig. 1. MR data sets of different patients: normal landmarks, quasi-landmarks, and estimated error ellipses (enlarged by a factor of 7).

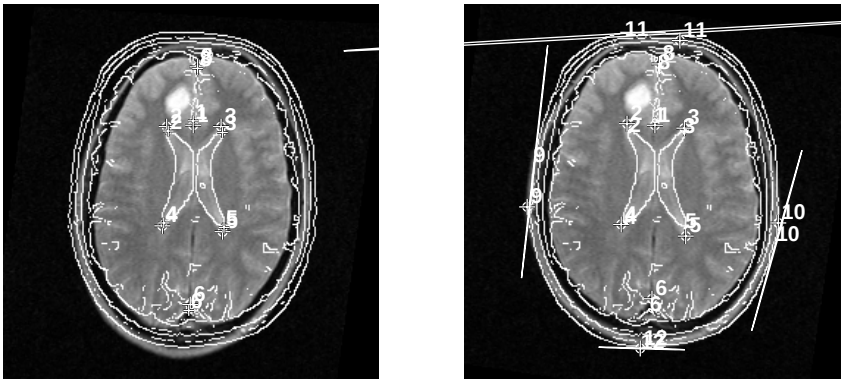

Fig. 2. Registration results: Thin-plate spline approximation using normal landmarks along with equal scalar weights (left), and using normal landmarks, quasi-landmarks and estimated covariance matrices (right).

the first image and have overlayed it onto the computed edges of the second image. While the registration accuracy within the inner parts of the brain is quite good, at the outer parts there are larger errors. If instead we use both the normal landmarks and the quasi-landmarks while incorporating anisotropic errors, then we can significantly improve the registration accuracy as shown in Fig. 2 on the right.

With the second example we demonstrate the usefulness of incorporating orientation attributes at landmarks. With the two synthetic images in Fig. 3 we simulate the rotation of a rigid structure (such as bone) embedded in an otherwise elastic material. If we use point landmarks only (four landmarks at the rigid structure and four landmarks at the image corners), then we obtain the result shown in Fig. 4 on the left. We see that the whole image including the rigid structure is elastically deformed. Next, we have incorporated orientations

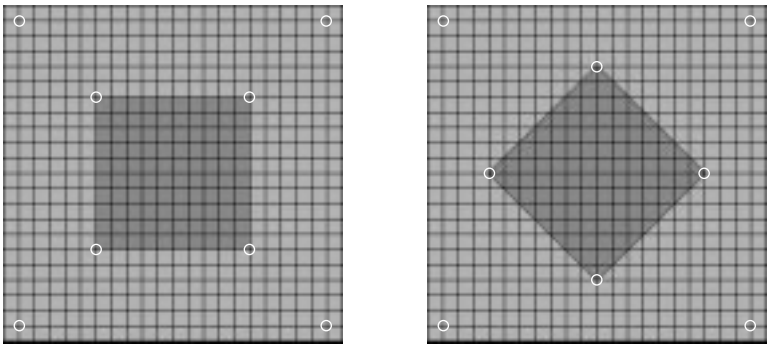

Fig. 3. Synthetic images simulating the rotation of a rigid structure in an otherwise elastic material.

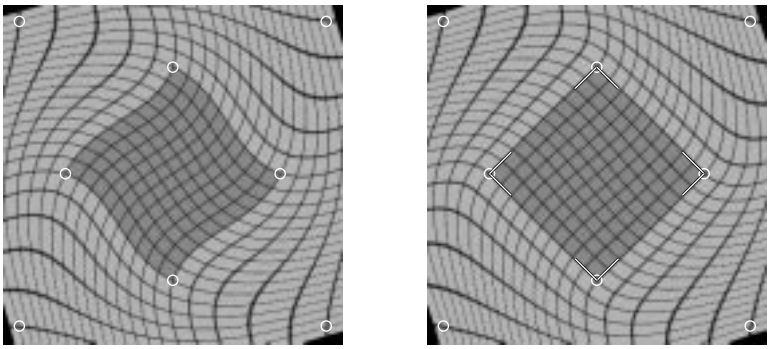

Fig. 4. Registration results: Interpolating thin-plate splines using only point landmarks (left) and incorporation of orientations at landmarks (right).

at the landmarks of the rigid structure. In all our experiments incorporating orientations we used $c = 1$ and $m = 2$ for the functional in (6). At each of the four landmarks of the rigid object in Fig. 3 we have specified two orientations which are aligned with the contours of the object. Using this additional knowledge for image registration significantly improves the result, i.e., the shape of the rigid object is well preserved (Fig. 4 on the right). Previously, Little et al. [14] have considered the problem of preserving rigid structures within elastic material. However, in their approach a full segmentation of the rigid structures is necessary. With our scheme we neither needed a full segmentation nor have we needed additional point landmarks.

In the third example we treat the case of several rigid structures embedded in elastic material. Fig. 5 shows two synthetic images that simulate the bending of a spine which is represented by five rigid components (see also [14]). The registration result in Fig. 6 on the left is obtained if we apply interpolating thin-plate splines while using four landmarks for each rigid component as well as four image border landmarks. In Fig. 6 in the middle the result is shown if we include

two orientations at each landmark of the rigid components, while still applying an interpolation scheme. It can be seen that the shape of the rigid structures is better preserved, particularly the outer contours of the rigid components are not curved as in the case of using point landmarks only. A further improvement is obtained if we use both the point landmarks and the orientations but apply an approximation scheme (Fig. 6 on the right). Here we have used equal isotropic landmarks errors in the functional in (6). From the result it can be seen that the contours of the rigid components are straight and now also the gridlines within the rigid components are nearly straight. Thus the shape of the rigid structures is better preserved.

With the last example we show an application where we have integrated both anisotropic landmark errors and orientation attributes. In Fig. 7 two MR images of different patients are shown. We have selected normal point landmarks and quasi-landmarks, and we have estimated the error ellipses directly from the image data. If we use only the normal landmarks (9 landmarks; Nr. 1,2,4,7,10,11,16,17,18) and apply interpolating thin-plate splines, then we obtain the result shown in Fig. 8 on the left. Deviations can be observed in the regions where no landmarks have been specified, particularly at the upper part of the brain and at the corpus callosum. Next, we have used the normal landmarks from above together with three quasi-landmarks at the skin contour (landmarks Nr. 25,26,27). For all landmarks we have automatically estimated the covariance matrices and we have applied the approximating thin-plate spline approach incorporating anisotropic errors. From Fig. 8 on the right it can be seen that the registration accuracy at the upper part of the brain is now much better while at the corpus callosum there is still a larger deviation. We can further improve the result in this region if we additionally integrate orientations at landmarks. In this example, we have included one orientation at landmark Nr. 1 (genu of corpus callosum). In both images this orientation points to the top of the corpus callosum. From Fig. 9 we see, that we now obtain a significantly better registration accuracy of the whole corpus callosum.

5 Summary and Future Work

In this contribution, we have proposed an approach to elastic registration of medical images that is based on point landmarks and additional attributes. Our scheme is based on a minimizing functional which covers the full range from interpolation to approximation. Since the solution can be stated analytically we yield an efficient computational scheme. Central to this work is the integration of anisotropic landmark errors and orientation attributes at landmarks. By this we incorporate statistical as well as geometric information as additional knowledge in elastic image registration. We have demonstrated that this additional knowledge can significantly improve the registration result. In particular, we have shown that by incorporating orientation attributes it is possible to preserve the shape of rigid structures (such as bone) in an otherwise elastic material. This can

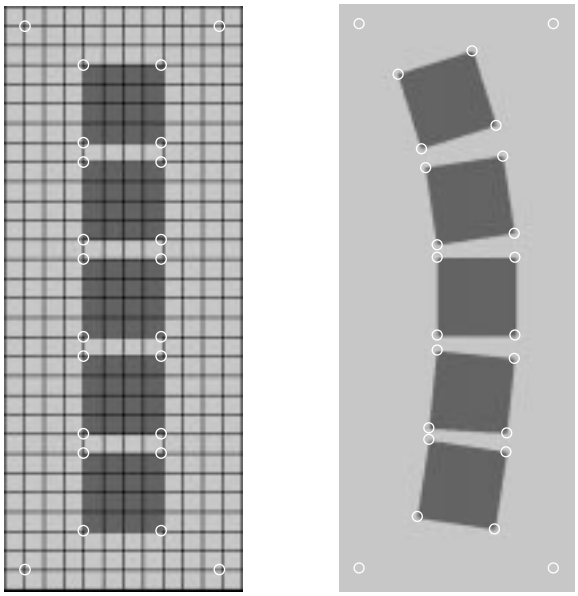

Fig. 5. Synthetic images simulating a spine that is bended.

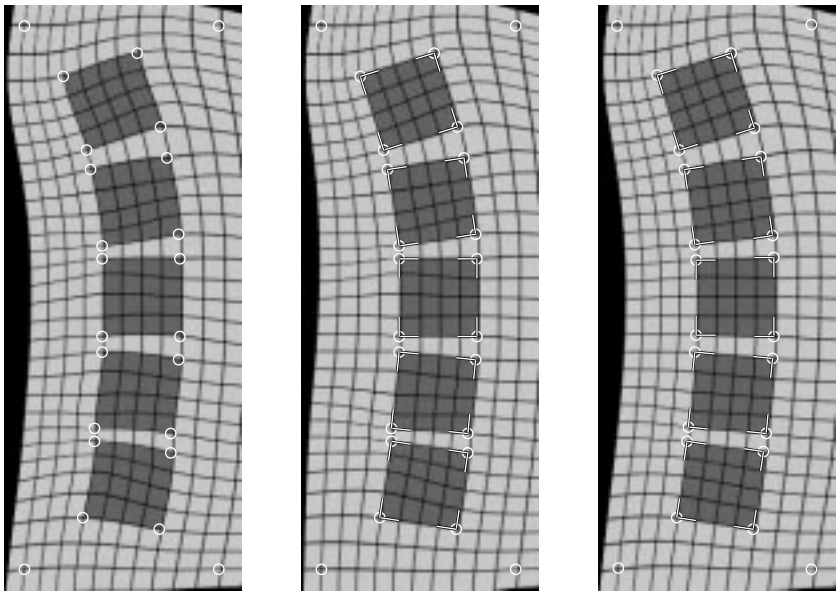

Fig. 6. Registration results: Interpolating thin-plate splines using only point landmarks (left), integration of two orientations at each object landmark (middle), and approximating thin-plate splines using point landmarks and orientations (right).

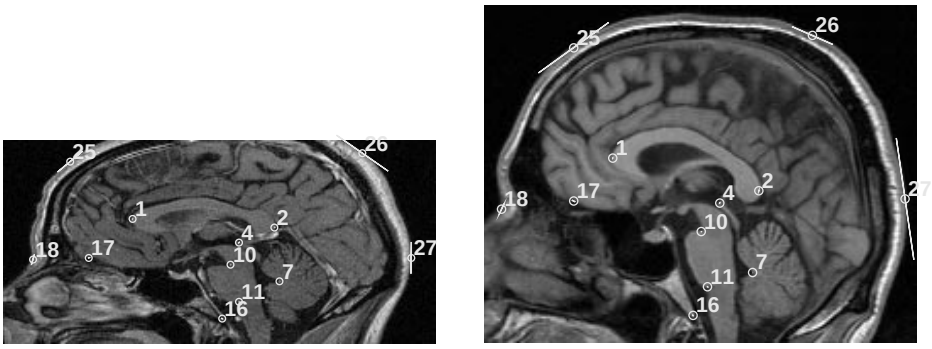

Fig. 7. MR images of different patients: normal landmarks, quasi-landmarks, and estimated error ellipses.

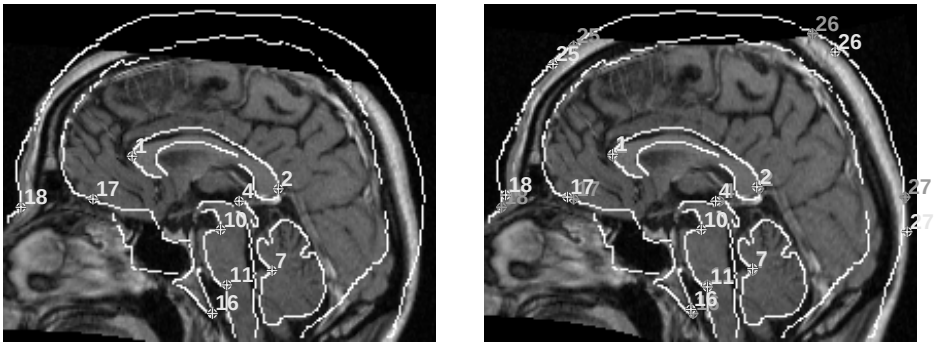

Fig. 8. Registration results: Interpolating thin-plate splines using normal landmarks (left), and approximating thin-plate splines using normal landmarks, quasi-landmarks and estimated covariance matrices (right).

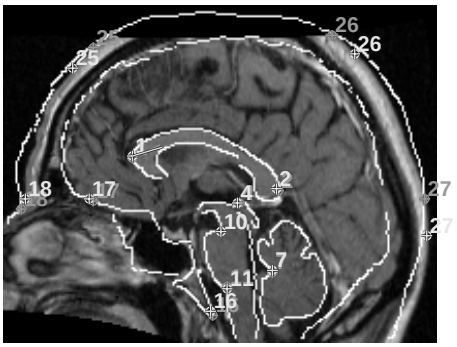

Fig. 9. Registration result: Approximating thin-plate splines using normal landmarks, quasi-landmarks, estimated covariance matrices, and orientations.

be achieved without selecting further landmarks and without a full segmentation of the rigid structures.

One problem with our approach is that the influence of incorporated orientations is rather global, i.e., image parts farer away from the positions of added orientations are often strongly affected, which is generally not desired. This observation has already been made earlier (see Mardia et al. [12]). In future work, means have to be found to constrain this global influence. Another topic for further research is the automatic estimation of the orientation attributes. While for rigid structures within elastic material the local orientation of the contour seems to be quite appropriate, for elastic material other choices which rather reflect the global geometry of anatomical structures, seem to be better suited.

Acknowledgement

This work has been supported by Philips Research Hamburg, project IMAGINE (IMage- and Atlas-Guided Interventions in NEurosurgery). We thank R. Sprengel for his contribution to this work. The original MR images have kindly been provided by Philips Research Hamburg and W.P.Th.M. Mali, L. Ramos, and C.W.M. van Veelen (Utrecht University Hospital) via ICS-AD of Philips Medical Systems Best.

References

1. Abbey, C.K., Clarkson, E., Barrett, H.H., Müller, S.P., and Rybicki, F.J.: A method for approximating the density of maximum-likelihood and maximum *a posteriori* estimates under a Gaussian noise model. Medical Image Anal. 2:4 (1998) 395-403
2. Bookstein, F.L.: Principal Warps: Thin-Plate Splines and the Decomposition of Deformations. IEEE Trans. on Patt. Anal. and Mach. Intell. 11:6 (1989) 567-585
3. Bookstein, F.L.: Four metrics for image variation. Proc. Int. Conf. Information Processing in Medical Imaging (IPMI'89), In: Progress in Clinical and Biological Research, Vol. 363, D. Ortendahl and J. Llacer (Eds.), Wiley-Liss New York, 1991, 227-240
4. Bookstein, F.L.: Landmark methods for forms without landmarks: morphometrics of group differences in outline shape. Medical Image Analysis 1:3 (1996/7) 225-243
5. Bookstein, F.L., and Green, D.K.: A Feature Space for Edgels in Images with Landmarks. J. of Mathematical Imaging and Vision 3 (1993) 231-261
6. Christensen, G.E., Joshi, S.C., and Miller, M.I.: Volumetric Transformation of Brain Anatomy. IEEE Trans. on Medical Imaging 16:6 (Dec. 1997) 864-877
7. Davis, M.H., Khotanzad, A., Flamig, D.P., and Harms, S.E.: A Physics-Based Coordinate Transformation for 3-D Image Matching. IEEE Trans. on Medical Imaging 16:3 (1997) 317-328
8. Duchon, J.: Interpolation des fonctions de deux variables suivant le principe de la flexion des plaques minces. R.A.I.R.O. Analyse Numérique 10:12 (1976) 5-12
9. Evans, A.C., Dai, W., Collins, L., Neelin, P., and Marrett, S.: Warping of a computerized 3-D atlas to match brain image volumes for quantitative neuroanatomical and functional analysis. Medical Imaging V: Image Processing, 1991, San Jose, CA, Proc. SPIE 1445, M.H. Loew (Ed.), 236-246

10. Fornefett, M., Rohr, K., Sprengel, R., and Stiehl, H.S.: Elastic Medical Image Registration using Orientation Attributes at Landmarks. Proc. Medical Image Understanding and Analysis (MIUA'98), Leeds/UK, 6-7 July 1998, E. Berry, D.C. Hogg, K.V. Mardia, and M.A. Smith (Eds.), Univ. Print Services Leeds 1998, 49-52
11. Mardia K., and Little, J.: Image warping using derivative information. In: Mathematical Methods in Medical Imaging III, 25-26 July 1994, San Diego, CA, Proc. SPIE 2299, F.L. Bookstein, J. Duncan, N. Lange, and D. Wilson (Eds.), 16-31
12. Mardia, K., Kent, J.T., Goodall, C.R., and Little, J.: Kriging and splines with derivative information. Biometrika 83:1 (1996) 207-221
13. Leamer, E.E.: Specification Searches – Ad Hoc Inferences with Nonexperimental Data. John Wiley & Sons New York Chichester 1978
14. Little, J.A., Hill, D.L.G., and Hawkes, D.J.: Deformations Incorporating Rigid Structures. Computer Vision and Image Understanding 66:2 (1997) 223-232
15. Maintz, J.B.A., and Viergever, M.A.: A survey of medical image registration. Medical Image Analysis 2:1 (1998) 1-36
16. Meyer, C.R., Boes, J.L., Kim, B., Bland, P.H., Zasadny, K.R., Kison, P.V., Koral, K., Frey, K.A., and Wahl, R.L.: Demonstration of accuracy and clinical versatility of mutual information for automatic multimodality image fusion using affine and thin-plate spline warped geometric deformations. Medical Image Analysis 1:3 (1996/7) 195-206
17. Rohr, K., Stiehl, H.S., Sprengel, R., Beil, W., Buzug, T.M., Weese, J., and Kuhn, M.H.: Point-Based Elastic Registration of Medical Image Data Using Approximating Thin-Plate Splines. Proc. Int. Conf. Visualization in Biomedical Computing (VBC'96), Hamburg, Germany, Sept. 22-25, 1996, Lecture Notes in Computer Science 1131, K.H. Höhne and R. Kikinis (Eds.), Springer Berlin 1996, 297-306
18. Rohr, K., Sprengel, R., and Stiehl, H.S.: Incorporation of Landmark Error Ellipsoids for Image Registration based on Approximating Thin-Plate Splines. Proc. Computer Assisted Radiology and Surgery (CAR'97), Berlin, Germany, June 25-28, 1997, H.U. Lemke, M.W. Vannier, and K. Inamura (Eds.), Elsevier Amsterdam Lausanne 1997, 234-239
19. Rohr, K.: Image Registration Based on Thin-Plate Splines and Local Estimates of Anisotropic Landmark Localization Uncertainties. Proc. Int. Conf. on Medical Image Computing and Computer-Assisted Intervention (MICCAI'98), Cambridge/MA, USA, Oct. 11-13, 1998, Lecture Notes in Computer Science 1496, W.M. Wells, A. Colchester, and S. Delp (Eds.), Springer Berlin 1998, 1174-1183
20. van Trees, H.L.: Detection, Estimation, and Modulation Theory, Part I. John Wiley and Sons, New York London 1968
21. Wahba, G.: Spline Models for Observational Data. Society for Industrial and Applied Mathematics, Philadelphia, Pennsylvania, 1990
22. Wahba, G.: Multivariate Function and Operator Estimation, Based on Smoothing Splines and Reproducing Kernels. In: Nonlinear Modeling and Forecasting, SFI Studies in the Sciences of Complexity, Vol. XII, M. Casdagli and S. Eubank (Eds.), Addison-Wesley 1992, 95-112
23. Wang, Y.: Smoothing Spline Models With Correlated Random Errors. J. of the American Statistical Association 93:441 (1998) 341-348